

나노결정립을 첨가한 비정질 금속에서의 전단띠 현상 Shear Band Generation in Amorphous Alloy with Distributed Nanocrystals

#박준영¹

*#J. Park(pcello@kumoh.ac.kr)¹

¹ 금오공과대학교 기계공학과

Key words : Shear band, Nanocrystals, Atomic strain

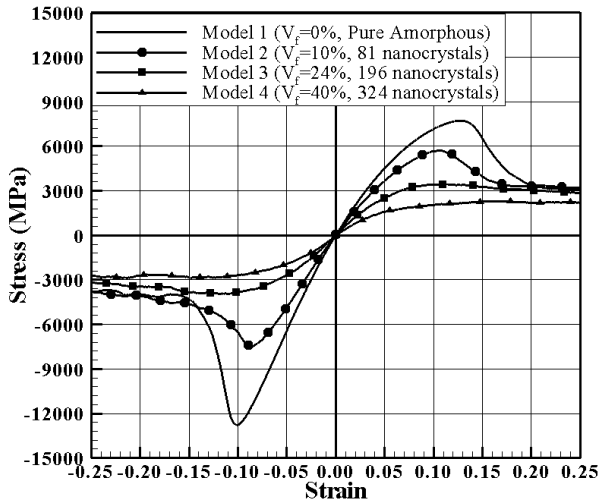


Fig. 1. Stress-Strain curve for the models with the different volume fraction of crystals.

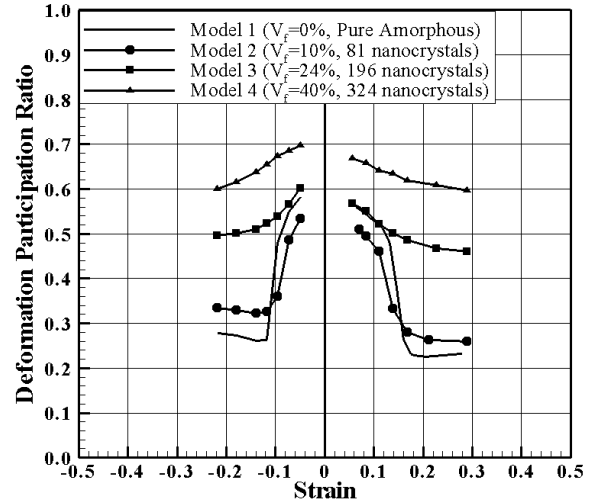


Fig. 2. Curve for DPR. vs. Strain. The volume fraction is proportional to the DPR.

1. Introduction

The deformation of metallic glasses is mainly driven by inhomogeneous deformation, a kind of strain localization called shear band. Except at temperature sufficiently high to allow homogeneous deformation, shear bands are directly related to strength and fragility of metallic glasses. Unstable and abrupt failure due to few shear bands is usually found on uniaxial tensile test while multiple shear bands showing apparently plastic deformation occur on uniaxial compression test or bending test [1-4]. It is important to understand the mechanism of shear band formation since abrupt failure is related to fragility prevents amorphous materials from being used in industrial applications.

In order to avoid the fragility, a lot of experimental researches have been investigated up to date on amorphous composite materials containing nanocrystals [3]. It is also reported that crystalline phases in metallic glasses enhance ductility or plastic strain up to 35%, because the crystalline phases can promote multiple shear bands [1-4]. Ironically, nanocrystals embedded by metallic glasses promote shear band formation and terminates within themselves. It means the nanocrystalline not only enhances the generation of shear band, but also prevents the propagation of shear band. It is believed that this dual nature is why the amorphous composite materials with nanocrystals have more ductility.

2. Computational Model

The 100,000-atoms Cu57Zr43 system with pure amorphous structure is chosen as a representative model (Model 1). The fully relaxed model with the size of about 31nm×31nm×17nm employs molecular dynamics study using modified Lennard-Jones potential

fitted to the amorphous Cu57Zr43 system, in plane stress condition [5].

To make the amorphous composite materials with nanocrystals, we insert the nanostructures artificially with the perfect Zr2Cu crystal structure usually found in experimental studies [6] and the size of about 1nm×1nm, into model 1. The different numbers of nanocrystals are evenly distributed into the already-made amorphous structure before the relaxation: model 2 with 81 crystals corresponding to about 10%, model 3 with 196 crystals corresponding to about 24% and model 4 with 324 crystals corresponding to 40%. To make shear band, uniaxial tension and uniaxial compression are applied to each model. Deviatoric atomic strain is quantified by the atomic strain definition suggested by Mott and Argon [7]. In order to quantify the degree of strain localization, i.e. shear band, a quantity called deformation participation ratio (DPR) introduced by Shi and Falk is utilized [8]. The definition of DPR is the fraction of atoms that have an atomic deviatoric shear strain larger than that of the whole system. As the strain becomes localized, the DPR should be small.

3. Results and Discussion

As shown at Figure 1, the models with low volume fraction of nanocrystal reach to a maximum stress corresponding to 0.1 strain then suddenly drops during uniaxial loadings. Unlike those with low volume fraction, the models with high volume fraction show a typical stress-strain curve shape of crystalline materials, i.e. there are no overshoots on stress-strain curve for high volume fraction of nanocrystals. It means that yield point decreases as volume fraction of nanocrystal increases. Finally, the overshoot diminishes at high volume fractions. We also found that the point with maximum stress is corresponding to the onset of shear band.

In order to measure the degree of strain localization, the curves

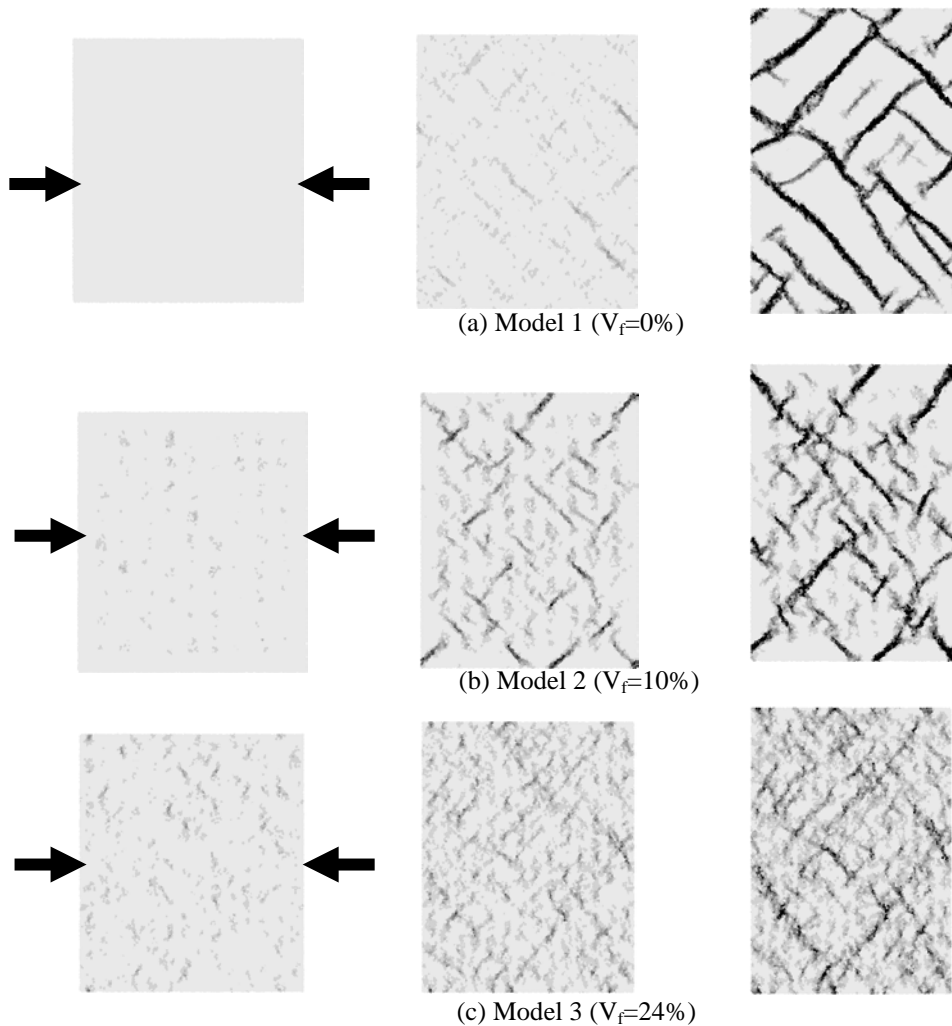


Fig. 3 Shear bands represented by the deviatoric shear strain of uniaxial compression for each model, from left to right with $\epsilon_{11} = -0.05, -0.10$ and -0.15 . Atoms are colored according to the value of the atomic deviatoric shear strain. Black represents a strain greater than 0.1 while white represents 0.0 strain.

for DPR are depicted at Figure 2. While the models 1 and 2 with low volume fraction of nanocrystals have sudden drops at around 0.1 strain corresponding to the maximum stress and the onset of shear band, the models 3 and 4 do not show sudden drops. It means there is no severe strain localization at these models. While the magnitudes of flow stresses in Figure 1 show relatively small differences, the DPRs show large differences in Figure 2. It means that the strain localization can be prevented without a severe drop of flow stress. As seen in Figure 2, the model 3 and 4 do not show any sudden drop. The DPRs is continually decreasing during the deformation.

Figure 3 depicts the strain states of each model in compression test. Like the cases of tension, model 1 and 2 shows clear shear bands corresponding to sudden drops of DPRs and stress. The deformations of model 3 and 4 also seem to be a homogenous deformation rather than strain localization. However, the number of shear band found in the model 1 and 2 is relatively greater than that of tension as found in the experimental studies [1].

4. Conclusion

Consequently, amorphous materials with high volume fraction of nanocrystals make homogeneous deformation during tension or compression without large decrease of flow stress. The DPRs also depict the improved states, i.e. no sudden drop and relatively high

values. The strain state during the deformation represents a few shear bands at low volume fraction while there are no distinguishable shear bands at high volume fraction of nanocrystals.

Acknowledgement

This paper was supported by Research Fund, Kumoh National Institute of Technology

Reference

1. Hays C.C., Kim C.P., and Johnson W.L.: Phys. Rev. Lett. 84 (2000) 2901
2. Fan C. and Inoue A.: Appl. Phys. Lett. 77 (2000) 46-48
3. Kato H., Hirano T., Matsuo A., Kawamura Y. and Inoue A.: Scripta Mater. 43 (2000) 503-507
4. Jiang W.H. and Atzmon M.: Scripta Mater. 54 (2006) 333-336
5. Kobayashi S. and Maeda K. and Takeuchi S.: Acta Metall. 28 (12) (1980) 1641-1652
6. Xing L. Q., Eckert J., Loser W. and Schultz L.: Applied Physical Letters 74(5) (1999) 664-666
7. Mott P. H., Argon A. S. and Suter U. W.: J. Comput. Phys. 101 (1992) 140-150.
8. Shi Y. and Falk M.: Phys. Rev. B 73 (2006) 214201-1~10